Hydrol. Earth Syst. Sci., 18, 1979–1994, 2014
www.hydrol-earth-syst-sci.net/18/1979/2014/
doi:10.5194/hess-18-1979-2014

Hydrology and Earth System Sciences
Open Access

Attribution of climate change, vegetation restoration, and engineering measures to the reduction of suspended sediment in the Kejie catchment, southwest China

X. Ma[1,2,3], X. X. Lu[4], M. van Noordwijk[5], J. T. Li[6], and J. C. Xu[1,2]

[1]Center for Mountain Ecosystem Studies, Kunming Institute of Botany, Kunming, 650204 China
[2]World Agroforestry Centre, East and Central Asia Region, Kunming, 650204 China
[3]Yunnan Institute of Environmental Sciences, Kunming, 650034 China
[4]Department of Geography, National University of Singapore, 117570 Singapore
[5]World Agroforestry Centre, Southeast Asia, Bogor 16001, Indonesia
[6]Baoshan Water Resource and Hydrological Bureau, Baoshan, 678000 China

Correspondence to: J. C. Xu (j.c.xu@cgiar.org)

Received: 19 August 2013 – Published in Hydrol. Earth Syst. Sci. Discuss.: 15 October 2013
Revised: 10 March 2014 – Accepted: 8 April 2014 – Published: 26 May 2014

Abstract. Suspended sediment transport in rivers is controlled by terrain, climate, and human activities. These variables affect hillslope and riverbank erosion at the source, transport velocities and sedimentation opportunities in the river channel, and trapping in reservoirs. The relative importance of those factors varies by context, but the specific attribution to sediment transfer is important for policymaking, and has wide implications on watershed management. In our research, we analyzed data from the Kejie watershed in the upper Salween River (Yunnan Province, China), where a combination of land cover change (reforestation, as well as soil and water conservation measures) and river channel engineering (sand mining and check dam construction) interact with a changing climate. Records (1971–2010) of river flow and suspended sediment loads were combined with five land-use maps from 1974, 1991, 2001, 2006 and 2009. Average annual sediment yield decreased from 13.7 t ha^{-1} yr^{-1} to 8.3 t ha^{-1} yr^{-1} between the period 1971–1985 and the period 1986–2010. A distributed hydrological model (Soil and Water Assessment Tools, SWAT) was set up to simulate the sediment sourcing and transport process. By recombining land-use and climate data for the two periods in model scenarios, the contribution of these two factors could be assessed with engineering effects derived from residual measured minus modeled transport. Overall, we found that 47.8 % of the decrease was due to land-use and land cover change, 19.8 % to climate change, resulting in a milder rainfall regime, 26.1 % to watershed engineering measures, and the remaining 6.3 % was due to the simulation percent bias. Moreover, mean annual suspended sediment yield decreased drastically with the increase of forest cover, making diverse forest cover one of the most effective ecosystems to control erosion. For consideration of stakeholders and policymakers, we also discuss at length the modeling uncertainty and implications for future soil and water conservation initiatives in China.

1 Introduction

Sediment transport in rivers can be a symptom of systemic erosion problems, but it also increases with landslides (natural or unnatural), riverbank instability, and human disturbances such as (road) construction and mining activities (Verbist et al., 2010). Walling and Fang (2003) found that among 145 rivers in a global data set on annual sediment loads, 4.8 % (7 rivers) had an increased load, 49.3 % (70 rivers) were stable, and 46.9 % (68 rivers) had a decreased load, probably mostly due to reservoir construction. Liu et al. (2008) similarly classified the 10 major rivers in China, and found 7 with decreasing sediment and stable runoff, 1 with decreasing sediment and runoff, and 2 with significant decreases in sediment and runoff. Dai et al. (2009)

reported that the decadal suspended sediment flux decreased by 70.2 % from 1.81 Gt yr^{-1} for 1954–1963 to 0.54 Gt yr^{-1} for the period 1996–2005 in nine major rivers in China.

Soil erosion is caused by the interaction between climate (especially rainfall intensity, amount, and distribution), terrain properties, and human activities (Dai et al., 2009), and results in a major loss of natural capital (Pimentel, 2006). Vegetation restoration (i.e., tree planting, grass establishment, and ecological restoration measures) and engineering measures (i.e., terrace and silt check dams) are commonly employed for erosion control in China (Huang and Zhang, 2004). The relative contribution of these measures is a debated issue and may depend on local context.

Check dams were identified as the most effective short-term measure for reducing coarse sediment entering the Yellow River (Ran et al., 2008; Xu et al., 2004; Xu et al., 2013). Reservoirs can intercept most of the suspended sediments and override any effect of erosion reduction (Rijsberman and Wolman, 1985). In fact, over the past 20 years, vegetation-based soil and water conservation has had a negligible effect on sediment loads in several large rivers in China, but they may have reduced the rate at which reservoirs fill. This includes in the Pearl River (Wu et al., 2012), contributing only 9.2 % to the reduction of sediment load in the downstream Miyun reservoir in Beijing (Tang et al., 2011), with less than 15 % reduction in the Three Gorges Reservoir (Xiong et al., 2009) and Yangtze River (Dai et al., 2008). However, Wang et al. (2007b) found that soil conservation measures were responsible for 40 % of the total sediment load decrease in the Yellow River basin. Yet, the relationship between forest cover and soil erosion is complex (Ran et al., 2013), as the litter layer and understory vegetation – which exert primary control – vary with forest, vegetation type, and management (Hairiah et al., 2006). A diverse and mixed forest cover may be the most effective variable for controlling erosion (Men, 2011). However, until now, none of these studies have considered the impacts of climatic variation and change, which likely interact with the roles of vegetation, increasing or decreasing erosion.

In light of the alternative solutions for controlling sediment loading in streams, it is important to understand the role of vegetation restoration and engineering measures previously undertaken for erosion control. In recent decades, there has been little change in average annual runoff; however, we have seen a dramatic decrease in annual sediment yield. Consequently, since there is currently no widely accepted method for attributing the decline of sediment yield to land-use and land cover change, engineering efforts, as well as climate change, we set out to explore a modeling approach in which land cover effects, climate, and engineering impacts can each be separated by recombination.

In this research, we examined the Kejie watershed region in China's southwest Yunnan Province because of its importance as a key watershed protection area and focus of soil conservation zone planning. The objective of this article is to (1) use the data available for the Kejie watershed to calibrate and validate a hydrological model (SWAT) with uncertainty analysis using the SUFI-2 algorithm, and (2) quantify the contribution of climate change, vegetation restoration, and engineering measures to the recorded decrease in sediment load using the calibrated and validated model based on a time series of land-use maps.

2 Description of the watershed

The Kejie watershed in western Yunnan Province is an upstream watershed in the Salween Basin, and has a total area of 1755 km^2 (Fig. 1). The Donghe River, a major tributary of the upper Salween River, is the main watercourse and runs for 95 km, with an average slope of 11^0 (ranging from 1 to 88^0). The climate is sub-tropical in the valleys and temperate in mountain areas. The mean annual precipitation is 995 mm, with a recorded maximum of 1368 mm (2001) and minimum recorded precipitation of 663 mm (2009). More than 80 % of the precipitation occurs in the monsoon season, from May to October. Annual runoff varies between 3.3×10^8 m^3 (2005)and 11.0×10^8 m^3 (2001), with an average of 6.4×10^8 m^3. Effective water yield is 364 mm (188–627 mm) yr^{-1}. River flow data were analyzed by Ma et al. (2009a).

Administratively, the Kejie watershed covers most of Longyang County, and small parts of Shidian and Changning County–all in the Baoshan Prefecture. Baoshan is considered to be a key watershed protection area, important for downstream stakeholders (Fig. 1b). While 34 % of the total area in Yunnan Province is classified as being sensitive to soil erosion, 37 % of Baoshan Prefecture, and 49 % of Longyang County were classified as such in 2004 (Ma et al., 2009b). Of the total erosion-sensitive areas in Longyang County, 76.8 % was classified as medium erosion prone, 18.5 % as slightly erosion prone, and 4.7 % as a high-risk erosion area.

Landslides and small-scale mud–rock flows happen frequently in this area, with heavy damage to property and landscapes. Since the 1980s, many significant attempts have been made by the central and local government in China to combat soil erosion, with varying results. In recent decades, annual sediment yield has varied between 14.7×10^4 t (2005; 0.84 t ha^{-1} yr^{-1}) and 495.1×10^4 t (1985; 28.2 t ha^{-1} yr^{-1}), with an average of 173.0×10^4 t (9.86 t ha^{-1} yr^{-1}).

The predominant soil type in the region is red. The natural vegetation of semi-moist, broad-leaved forests disappeared many decades ago and has been replaced by conifer trees, with a mix of alder (*Alnus nepalensis*) and other broad-leaved forest species.

Operational since 1959, there is a middle-sized reservoir, called Beimiaoshuiku (with a capacity of 5.850×10^4 m^3), located in the upstream Donghe River (Fig. 1c). As the reservoir was operational before the start of our study period (1965) and its management has not undergone major change,

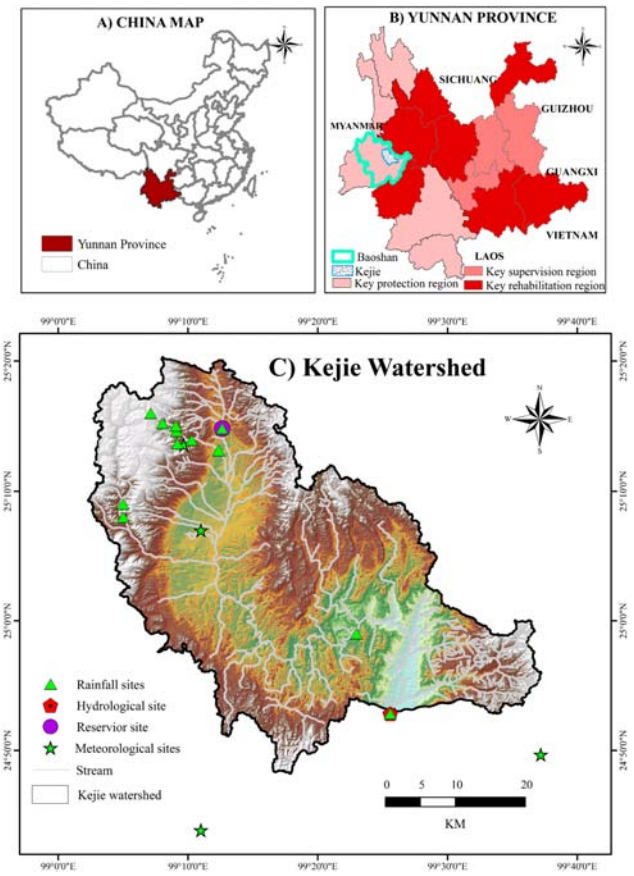

Figure 1. Location map of the Kejie watershed, in Yunnan Province, southwest China, with current erosion classification of the province (Fig. 1b), location of weather and rainfall stations, and catchment outflow.

its main effect in this study was as a constant sediment trap for its upstream area.

3 Materials and methods

3.1 Available materials

3.1.1 Hydro-meteorological data sets

Three meteorological stations with long-term data records (1965–2010) in, or adjacent to, the Kejie watershed, and one with short-term records (1998–2002) in the Xizhuang sub-watershed, were available. The daily values of six parameters were collected, including rainfall, maximum temperature, minimum temperature, wind speed, relative humidity, and sunshine hours. In addition, two rainfall stations with long-term daily rainfall data in the Kejie watershed (1965–2010), and seven rainfall stations with short-term daily rainfall data in the Xizhuang sub-watershed (1998–2002), were available. One hydrological station with long-term daily discharge and suspended sediment data is located at the outlet of the Kejie watershed (1965–2010). One medium-sized reservoir, with long-term daily outflow readings is situated in the upper reaches of the Donghe River in the Kejie watershed (1965–2010). All hydro-meteorological data sets were provided by the Baoshan Department of Hydrology and Meteorology (Fig. 1c, Table 1).

3.1.2 Land-use maps

The soil map, digital elevation model (DEM), and vegetation/crop parameters were discussed by Ma et al. (2009a). Five land-use maps of the Kejie watershed were used to analyze land-use change over the past several decades. Maps for 1974, 1991, 2001 and 2006 were classified by Ma et al. (2009a), and an additional map for 2009 was obtained from the Baoshan Department of Forestry, based on a SPOT 5 image from 2009. As the classification of this 2009 map was more detailed than the previous maps, map units were combined to match the earlier map legends.

3.2 Change trend detection

Mann–Kendall's non-parametric test (Mann, 1945; Kendall, 1948) was performed alongside the parametric t test in the monotonic change trend detection for long-term records (van Belle and Hughes, 1984). This testing method has been extensively used with environmental time series (Burn et al., 2004; Ma et al., 2009a). For our purposes, we used this method here to identify the trend of runoff and the suspended sediment yield (SSY). Testing results were generated using the Kendall package in the R statistical analysis software program (Team, 2008).

The piecewise regression model is an effective tool for modeling abrupt thresholds. In a "broken-stick" model, two or more lines are joined at unknown point(s), called "breakpoint(s)" (Toms and Lesperance, 2003), and are widely used to identify ecological thresholds (Oswald et al., 2011; Zhang et al., 2013). A simple model with two straight lines joined sharply at the breakpoint – appropriate when there is an abrupt transition – was selected in this study and implemented in R (Team, 2008), with the following equations:

$$y_i = \begin{cases} \beta_0 + \beta_1 t_i + \varepsilon, t \le \alpha \\ \beta_0 + \beta_1 t_i + \beta_2 (t_i - \alpha) + \varepsilon, t > \alpha, \end{cases} \quad (1)$$

where y_i is the annual suspended sediment yield, t_i is the corresponding year, α is the turn-point (year), and β_0, β_1 and β_2 are regression coefficients. Furthermore, ε is the residual of the fit, and β_1 is the slope of the line before the turning point, whereas $\beta_1 + \beta_2$ is the slope after that point.

3.3 SWAT model description

In our analysis, we used the SWAT model – calibrated and validated with the Kejie watershed water balance data (Ma et

Table 1. Characteristics of hydro-meteorological stations in the Kejie watershed.

Site name	Latitude	Longitude	Elevation (m)	Period	Type
Baoshan	25°07′	99°11′	1652	1965–2010	Meteorological stations with 6 parameters
Changing	24°49′41″	99°37′12″	1658	1965–2010	
Ganwangkeng	25°13′32	99°09′41″	1955	1998–2002	
Shidian	24°43′51″	99°11′00″	1489	1965–2010	
Beimiaoshuiku	25°14′47″	99°12′38″	1730	1965–2005	Rainfall stations
Damaidi	25°15′11″	99°08′02″	2225	1998–2002	
Dawopo	25°13′37″	99°09′11″	2120	1998–2002	
Kejie	24°52′50″	99°25′36″	968	1965–2005	
Laishitou	25°15′58″	99°07′08″	3076	1998–2002	
Lijiasi	25°14′35″	99°09′07″	1970	1998–2002	
Qingshui	25°13′54″	99°10′17″	1852	1998–2002	
Shangoushui	25°15′00″	99°09′04″	2090	1998–2002	
Xizhuang	25°13′08″	99°12′22″	1705	1998–2002	
Kejie	24°52′50″	99°25′36″	968	1965–2010	Hydrological station
Baimiaoshuiku	25°14′47″	99°12′38″	1730	1965–2010	Reservoir outflow

al., 2009a) from 1971 to 1979 – to simulate the SSY under five different land-use maps. The SWAT model predicts long-term impacts of land use on water, sediment, and agricultural chemical yield in large complex watersheds with varying soils, land-use and management conditions (Arnold and Fohrer, 2005), and is widely used to simulate the SSY (Betrie et al., 2011; Cai et al., 2012; Oeurng et al., 2011; Qiu et al., 2012).

In SWAT, a watershed is divided into multiple sub-basins, which are further subdivided into hydrologic response units (HRU), consisting of uniform land cover, soil, and slope that drain directly to the sub-basin's channel. The hydrological modeling component in SWAT was previously discussed in Ma et al. (2009a). For soil erosion, it uses the Modified Universal Soil Loss Equation (MUSLE) developed by Williams and Berndt (1977). The MUSLE is

$$\text{sed} = 11.8 \times (Q_{\text{surf}} \times q_{\text{peak}} \times \text{area}_{\text{hru}})^{0.56} \times K_{\text{USLE}} \times C_{\text{USLE}} \times P_{\text{USLE}} \times \text{LS}_{\text{USLE}} \times \text{CFRC}, \quad (2)$$

where sed is the sediment yield (metric t day^{-1}), Q_{surf} is the surface runoff volume (mm ha^{-1} day^{-1}), q_{peak} is the peak runoff rate (m^3 s^{-1}), area_{hru} is the area of the HRU (ha), K_{USLE} is the USLE (Universal Soil Loss Equation) soil erodibility factor, C_{USLE} is the USLE cover and management factor, P_{USLE} is the USLE support practice factor, LS_{USLE} is the USLE topographic factor and CFRG is the coarse fragment factor.

The channel sediment routing equation uses a modification of Bagnold's sediment transport equation (Bagnold, 1977). Sediment deposition in the channel is based on stream power (Williams, 1980) and fall velocity related to particle size. Channel degradation is adjusted using USLE soil erodibility and channel cover factors (Arnold et al., 1995).

The ArcSWAT model version 2009.93.7b was run in an ArcGIS 9.3 interface, with basic parameters as described by Ma et al. (2009a). The watershed was divided into 45 sub-basins, while the number of HRUs varied depending on the land cover map (353 for the 1974 map) in the SWAT model. Since observed sediment data was not complete in 1967, and the data in 1970 was missing, the simulation period of 1965–1970 was treated as a "warming up" period for the model to obtain a reasonable initial value for each of the variables.

3.4 Calibration setup and analysis

The SWAT model was calibrated and validated for streamflow and SSY in the Kejie watershed. Monthly discharge and SSY records from 1971 to 1980 at the outlet of the watershed (the Kejie hydrological station) were split into two segments, 1971–1975 and 1976–1980, in order to calibrate and subsequently validate water and sediment-relative parameters. Both manual calibration and auto-calibration were used in our study. By comparing the simulated monthly streamflow/SSY (default parameter) with the observed streamflow/SSY, the water and sediment-relative parameters were calibrated manually. Then the pre-calibrated parameters were refined through auto-calibration.

SWAT Calibration and Uncertainty Procedures (SWAT-CUP) software was selected to do the auto-calibration because of its capability to perform calibration, validation, sensitivity analysis and uncertainty analysis – and also because its performance was better than the auto-calibration modulus embedded in the SWAT interface (Zhou et al., 2014).

The SWAT-CUP program contains different algorithms, including: Sequential Uncertainty Fitting (SUFI-2), Particle Swarm Optimization (PSO), Generalized Likelihood Uncertainty Estimation (GLUE), Parameter Solution (ParaSol), and Markov Chain Monte Carlo (MCMC). Compared with other algorithms, SUFI-2 has a higher efficiency in achieving a similarly accurate predication result, which has been widely used to model streamflow, sediment load, and water quality in recent years (Abbaspour et al., 2007, 2009; Azimi et al., 2013; Faramarzi et al., 2009; Schuol et al., 2008a, b). So SUFI-2 was selected to auto-calibrate the streamflow and SSY in the Kejie watershed.

3.4.1 Parameter sensitivity

Sensitivity analysis is important to help identify the parameters most significantly influencing the model output. Sensitivity analysis from SUFI-2 provided partial information about the sensitivity of the objective function to model parameters. In our study, 20 water-related parameters (global parameters), along with 8 sediment-related parameters (6 global parameters, and 2 parameters with a separate value for each land use) with absolute minimum and maximum ranges in the SWAT model documents were selected to do sensitivity analysis separately. Table 2 illustrates the sensitivity ranking. A t test is used to identify the relative significance of each parameter: a t stat provides a measure of sensitivity (larger absolute values are more sensitive), and p values determine the significance of the sensitivity (a value close to zero has more significance).

In terms of water process, the most sensitive parameter was found to be a curve number (CN2), followed by the baseflow alpha factor (ALPHA_BF), deep aquifer percolation fraction (RCHRG_DP), threshold depth of water in the shallow aquifer for "revap" or percolation to the deep aquifer (REVAPMN), threshold depth of water in the shallow aquifer required for return flow (GWQMN), soil evaporation compensation factor (ESCO), and others. On the basis of the previous study in the Kejie watershed (Ma et al., 2009a), nine parameters were selected to calibrate water process, namely CN2, ALPHA_BF, RCHRG_DP, REVAPMN, GWQMN, GW_REVAP (groundwater "revap" coefficient: regulates the movement of water from the shallow aquifer to the root zone), GW_DELAY (groundwater delay time: lag between the time that water exits the soil profile and enters the shallow aquifer), ESCO, EPCO (plant uptake compensation factor).

In terms of sediment-related parameters, the two most sensitive parameters were found to be the peak rate adjustment factor for sediment routing in the sub-basin (ADJ_PKR) and the peak rate adjustment factor for sediment routing in the main channel (PRF), followed by the agricultural (AGRL) practice factor in the USLE equation (USLE-P_AGRL), the agricultural land cover factor in the USLE equation (USLE-C _AGRL), the channel erodibility factor (CH_COV1), the forest (FRST) practice factor in the USLE equation (USLE-P_FRST), the forest land cover factor in the USLE equation (USLE-C_FRST), and others. ADJ_PKR, PRF, CH_COV1, CH_COV2 (channel cover factor), SPCO (linear parameter for calculating the maximum amount of sediment that can be re-entrained during channel sediment routing), and SPEXP (exponent parameter for calculating sediment re-entrained in channel sediment routing) explain the channel erosion and sediment re-entrainment. USLE_P and USLE_C control the generation of sediment in HRU; the sensitivity differed from agricultural to settlement. From the sensitivity analysis, combined with other studies (Betrie et al., 2011; Cai et al., 2012; Oeurng et al., 2011; Qiu et al., 2012), 16 parameters were selected to calibrate the sediment process. In total, 25 parameters were selected for calibration and validation of streamflow and SSY.

3.4.2 Model calibration and validation

Following the manual calibration instruction in the SWAT model document (Neitsch et al., 2002), the streamflow was first calibrated by adjusting the nine parameters manually. When the streamflow calibration was finished, the sediment calibration was also run manually. The values of 25 parameters from the manual calibration (pre-calibration) provided more realistic initial values and ranges for auto-calibration in the SWAT-CUP software.

Two variables with 25 parameters – namely, streamflow and sediment – were calibrated together in the SUFI-2 program. The step-by-step process of the SUFI-2 algorithm was described by Abbaspour et al. (2007). In our study, the Nash-Sutcliffe coefficient (N_{SE}) was chosen as the objective function. The initial parameter ranges were set according to the pre-calibrated values. Similar to other studies, including Zhou et al. (2014), the number of simulations in each iteration was set at 1000. When finishing one iteration simulation, the parameter ranges were replaced by the new ranges from the SUFI-2 output. Subsequently, a new iteration was set up. After three iterations, better parameter ranges with the best fitting parameters were achieved. A thorough validation was carried out by updating the corresponding files, and performing one iteration with the same number of simulations as the calibration runs.

3.4.3 Model evaluation and uncertainty analysis

In terms of evaluation of the performance of the model, three indexes were used – which, as before, included the N_{SE} (Nash–Sutcliffe efficiency), the P_{BIAS} (percentage bias), and the R_{SR} (ratio of the root mean square error to the standard deviation of measured data) (Moriasi et al., 2007). Details can be found in Ma et al. (2009a).

Uncertainty in hydrological modeling stems from input data (such as rainfall and temperature), model structure, model parameters, and the measured data (such as discharge

Table 2. Parameters sensitivity results in the Kejie watershed.

Process	Parameters	*t* Stat	*p* Value	Rank
Streamflow	R__CN2.mgt	15.42	0.00	1
	V__ALPHA_BF.gw	6.97	0.00	2
	V__RCHRG_DP.gw	−6.09	0.00	3
	V__REVAPMN.gw	5.45	0.00	4
	V__GWQMN.gw	−5.29	0.00	5
	V__ESCO.hru	2.97	0.00	6
	V__SFTMP.bsn	−2.13	0.03	7
	V__CANMX.hru	−2.05	0.04	8
	V__TIMP.bsn	2.02	0.04	9
	V__SMFMX.bsn	1.88	0.06	10
	V__SMTMP.bsn	1.75	0.08	11
	V__GW_DELAY.gw	−1.73	0.08	12
	V__EPCO.hru	−1.67	0.95	13
	R__SOL_BD(1).sol	1.57	0.12	14
	V__CH_N2.rte	−1.47	0.14	15
	V__CH_K2.rte	−1.39	0.16	16
	V__GW_REVAP.gw	−1.14	0.26	17
	V__SOL_Z(1).sol	0.71	0.48	18
	R__SOL_K(1).sol	−0.71	0.48	19
	R__SOL_AWC(1).sol	0.49	0.62	20
Sediment	V__ADJ_PKR.bsn	−10.09	0.00	1
	V__PRF.bsn	−8.79	0.00	2
	V__USLE_P_AGRL.mgt	−8.13	0.00	3
	V__USLE_C{AGRL}.crop.dat	−7.75	0.00	4
	V__CH_COV1.rte	6.97	0.00	5
	V__USLE_P_FRST.mgt	−6.39	0.00	6
	V__USLE_C{FRST}.crop.dat	−5.96	0.00	7
	V__USLE_C{RNGE}.crop.dat	−4.17	0.00	8
	V__USLE_P_RNGE.mgt	−3.68	0.00	9
	V__CH_COV2.rte	1.20	0.23	10
	V__USLE_P_SWRN.mgt	−1.05	0.29	11
	V__SPEXP.bsn	−0.89	0.38	12
	R__USLE_C{URML}.crop.dat	0.68	0.50	13
	V__USLE_C{SWRN}.crop.dat	−0.45	0.65	14
	V__SPCON.bsn	−0.37	0.71	15
	V__USLE_P_URML.mgt	−0.22	0.82	16

Note: the *t* Stat provides a measure of sensitivity (larger absolute values are more sensitive); the *p* value determines the significance of the sensitivity (a value close to zero has more significance); "R_" and "V_" means relative change and a replacement to the initial parameter values, respectively; "AGRL", "FRST", "RNGE", "SWRN" and "URML" stands for cropland, forests, grassland, barren land and settlements, respectively.

and SSY). SUFI-2 aggregates all sources of uncertainty to the parameter ranges. Two indices were used to quantify the strength of a calibration/uncertainty analysis, namely the P-factor and the R-factor (Abbaspour et al., 2007). The P-factor is the percentage of measured data bracket by the 95 % prediction uncertainty (95PPU), and 95PPU is calculated at the 2.5 % and 97.5 % level of the cumulative distribution of an output variable through Latin hypercube sampling; disallowing 5 % of the very worst simulation results. The P-factor indicates the degree to which the model uncertainties are being accounted for. The R-factor is the average thickness of the 95PPU band, divided by the standard deviation of the measured data. It represents the width of the uncertainty interval, and should be as small as possible. Ideally, the performance of SUFI-2 is to bracket most of the measured data (the P-factor approaching 1) with the smallest possible uncertainty band (R-factor approaching 0).

3.5 Differentiating the effects of different controls

The calibrated and validated model was used to distinguish the effect of climate change, vegetation change, and engineering measures on suspended sediment yield by recombining climate and land cover data (Tang et al., 2011; Ma et al., 2009a).

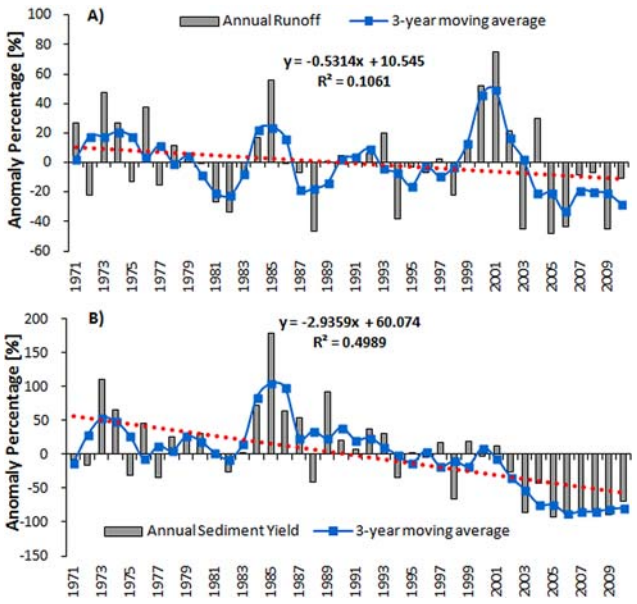

Figure 2. The trend and the inter-annual variability of annual runoff and suspended sediment yield in the Kejie watershed (1971–2010).

The observed change (Measured2 – Measured1) was partitioned using simulation results for various combinations of land cover (L) and climate (C) as follows:

$$\begin{aligned}\text{Change} &= \text{Measured2} - \text{Measured1}\\ &= (\text{Measured2-SimulatedL2C2})\\ &+ (\text{SimulatedL2C2-SimulatedL1C2})\\ &+ (\text{SimulatedL1C2-SimulatedL1C1})\\ &+ (\text{SimulatedL1C1-Measured1})\\ &= [\text{Engineering effects}]\\ &+ [\text{Land-use change effect}]\\ &+ [\text{Climate change effect}]\\ &+ [\text{Model bias}]. \end{aligned} \quad (3)$$

L1 stands for the land cover for Period 1 (1970–1985), which is represented by the 1974 land cover map. L2 stands for the land cover for Period 2 (1986–2010), which combined the 1991 land cover map (1986–1998), the 2001 map (1999–2002), and the 2009 map (2008–2010) into one cohesive map. C1 stands for the climate condition in Period 1, and C2 stands for the climate condition in Period 2. Simulation with land cover (L1) and climate condition (C1) (SimulatedL1C1) was the baseline simulation considering the physical conditions for Period 1; simulation with land cover (L1) and climate condition (C2) (SimulatedL1C2) was used to predict a "business-as-usual" scenario with the land cover kept constant into Period 2. Furthermore, simulation with land cover (L2) and climate condition (C2) (SimulatedL2C2) was used to provide a counterfactual scenario of what might happen in Period 2 without engineering measures, but with actual land cover for 1986 to 2010.

Consequently, (SimulatedL2C2-SimulatedL1C2) explained the effects from land-use change, while (SimulatedL1C2-SimulatedL1C1) explained the effects from climate change. (SimulatedL1C1-Measured1) expressed the minus simulation bias in Period 1. In terms of (Measured2-SimulatedL2C2), it can explain the effects from engineering measures, if the model simulation is without any bias. The percent bias of the simulation in Period 1 can be estimated from SimulatedL1C1 and Measured1. If we assumed the percent bias of the simulation in Period 2 was kept the same as Period 1, then the simulation bias in Period 2 could be successfully estimated. The effects of engineering measures can be estimated from (Measured2-SimulatedL2C2), minus the simulation bias in Period 2. [Model bias] was the difference between the simulation bias in Period 2 and in Period 1.

Table 3. Mann–Kendall trend tests of runoff and SSY in Kejie watershed; Tau is the Mann–Kendall rank correlation coefficient.

Type	Recorded year	Tau	2-sided p value
Runoff	1971–2010	−0.151	0.17283
SSY	1971–2010	−0.459	0.00003

Note: P represents annual rainfall; R-factor represents rainfall erosivity; SSY represents suspended sediment yield.

4 Results

4.1 Changing trends of suspended sediment yield

Annual runoff and SSY showed a declining trend from 1971 to 2010 (Fig. 2). The strongest and only statistically significant decrease was in SSY ($\alpha = 0.05$) (Table 3).

Within each decade the SSY was related to annual runoff, but the relationship as a whole shifted (Fig. 3). When compared at any given runoff rate, annual SSY increased from the 1970s to the 1980s – and then subsequently declined.

A piecewise regression model identified the breakpoint in recorded annual SSY to be the year 1985 (Fig. 4). Over the period 1971–1985, an increase was observed with a correlation coefficient of 0.29, which was not statistically significant (at $\alpha = 0.05$). Additionally, there was a decrease from 1986 to 2010, and a statistically significant correlation coefficient of 0.80 ($\alpha = 0.05$) was recorded. A similar pattern of sediment yield change was observed at the Yichang station on the Yangtze River (Dai et al., 2009).

Since the 1970s, many hillsides with vegetation had been converted to terraced fields to meet the food needs of an increasing population (Zhang et al., 1999). Road construction and other infrastructure development exacerbated soil

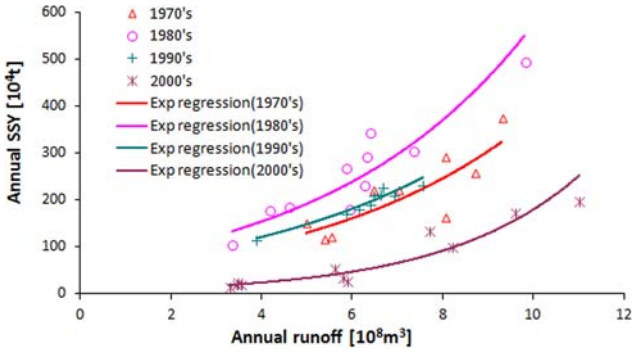

Figure 3. The relationship between annual runoff and suspended sediment yield at the outlet of the Kejie watershed (1971–2010).

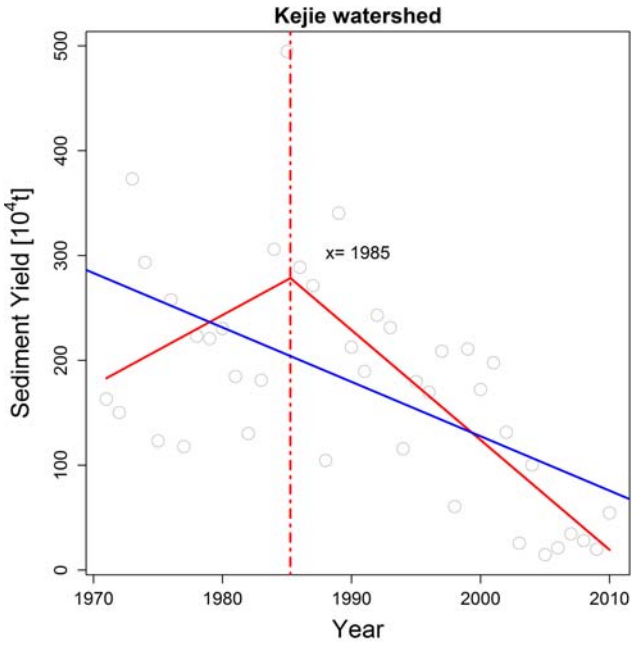

Figure 4. Change trend of suspended sediment yield in the Kejie watershed from 1965 to 2010 (red solid lines are the piecewise-regression lines; the blue solid line is the linear regression line; the red dashed line is to illustrate the breakpoint).

erosion during this period. In the 1980s, China made a transition from a "central planning" economy to a market economy. Measures were taken to rectify the erosion issues; steep slopes were reforested, and soil and water conservation programs, including ecological restoration, were rolled out. Engineering measures (terrace improvement, silt check dams) also contributed to the decrease of sediment yield in the watershed. Other human activities, including sand mining in the river (extraction of riverbed sediment) and riverbank protection, may have contributed to the decrease in sediment yield.

Using the breakpoint previously identified (1985), we divided the study period into two periods: (1) 1971–1985 and (2) 1986–2010. From Period 1 to Period 2, the mean annual

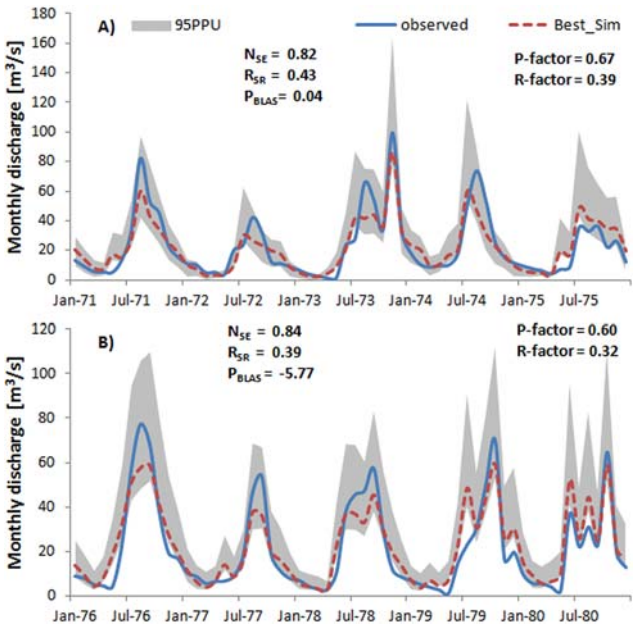

Figure 5. Comparison of the observed monthly discharge (blue bold line) and simulated monthly discharge (red dashed line) with 95 % prediction uncertainty band at the Kejie hydrological station. Calibration and validation results are shown in Fig. 5a and b.

runoff decreased by 10.8 %, and mean annual SSY decreased by 39.7 %. The magnitudes of change in runoff and sediment were apparently influenced by climate change, vegetation measures, and other engineering measures.

4.2 Model calibration and uncertainty measures

Table 4 listed the parameters in the last iteration of SUFI-2, their fitting values, and their final ranges. Figure 5a and b compared the monthly observed and simulated streamflow for the calibration and validation periods, respectively. The monthly simulated and observed discharge resulted in a very good model with $N_{SE} = 0.82$, $R_{SR} = 0.43$, and $P_{BLAS} = 0.04$ % in the calibration period; and with $N_{SE} = 0.84$, $R_{SR} = 0.39$, and $P_{BLAS} = -5.77$ % in the validation period. The observed total runoff volumes are captured well with a little underestimation (0.04 %) in the calibration period and a little overestimation (5.77 %) in the validation period. Compared with the manual calibration result by Ma et al. (2009a), the auto-calibration has improved the model performance, including the value of N_{SE} from 0.75 to 0.82 in the calibration period. It is worth noting that the simulation of the peak flows is a little weak. Generally speaking, the calibrated model can predict the monthly streamflow with accurate results.

Figure 6a and b illustrated the simulated and observed monthly SSY over the period 1971–1975 and 1976–1980, respectively. The simulated monthly SSY matches the observed values, with $N_{SE} = 0.74$, $R_{SR} = 0.51$,

Table 4. The final ranges and fitting values of the SWAT model parameters included in the final calibration procedure.

Parameters	Fitting value	Final parameter range	
		Min-value	Max-value
R__CN2.mgt	−0.033	−0.056	−0.006
V__ALPHA_BF.gw	0.031	0.030	0.032
V__RCHRG_DP.gw	0.026	0.010	0.087
V__REVAPMN.gw	49.8	29.9	61.7
V__GWQMN.gw	54.2	52.6	60.6
V__ESCO.hru	0.74	0.69	0.79
V__GW_DELAY.gw	67	66	72
V__EPCO.hru	0.67	0.63	0.71
V__GW_REVAP.gw	0.054	0.012	0.056
V__ADJ_PKR.bsn	0.696	0.654	0.783
V__PRF.bsn	0.377	0.000	1.222
V__CH_COV1.rte	0.40	0.33	0.43
V__CH_COV2.rte	0.43	0.00	0.60
V__SPEXP.bsn	1.256	1.234	1.701
V__SPCON.bsn	0.005	0.003	0.008
V__USLE_P_AGRL.mgt	0.580	0.525	0.617
V__USLE_P_FRST.mgt	0.199	0.148	0.244
V__USLE_P_RNGE.mgt	0.353	0.297	0.391
V__USLE_P_SWRN.mgt	0.624	0.573	0.624
V__USLE_P_URML.mgt	0.090	0.085	0.154
V__USLE_C{AGRL}.crop.dat	0.450	0.184	0.500
V__USLE_C{FRST}.crop.dat	0.167	0.010	0.309
V__USLE_C{RNGE}.crop.dat	0.011	0.010	0.323
R__USLE_C{URML}.crop.dat	0.332	0.146	0.436
V__USLE_C{SWRN}.crop.dat	0.291	0.134	0.399

and $P_{\mathrm{BLAS}} = 10.84\,\%$ in the calibration period, and with $N_{\mathrm{SE}} = 0.78$, $R_{\mathrm{SR}} = 0.47$, and $P_{\mathrm{BLAS}} = -1.48\,\%$ in the validation period. Likewise, the simulated month SSY cannot effectively capture the observed monthly peak values, which may have been caused by the empirical MUSLE model and the missing peak flow. However, in terms of the P_{BLAS}, the model can effectively capture the average SSY (underestimated by 10.84 % in the calibration period, and overestimated by 1.48 % in the validation period), which is more relevant to our study.

The uncertainty of the calibrated model in SUFI-2, 95PPUs, is the combination of the uncertainties in the input data, model structure, model parameters, and the measured data (which was not separately evaluated). The uncertainty was represented by the P-factor and the R-factor. In terms of monthly streamflow, the P-factor and the R-factor was 67 % and 0.39, 60 % and 0.32, respectively, for calibration and validation. This indicated about 67 % (60 %) (out of a perfect 100 %) of the measured monthly streamflow could be bracketed by the 95PPU with a very narrow 95PPU band of 0.39 (0.32) (close to a perfect 0) in the calibration (validation) period (Fig. 5a and b). In terms of monthly SSY, the P-factor and the R-factor were 87 % and 1.36, 87 % and 1.10, respectively, for calibration and validation. This indicated about 87 % (close to a perfect 100 %) of the measured

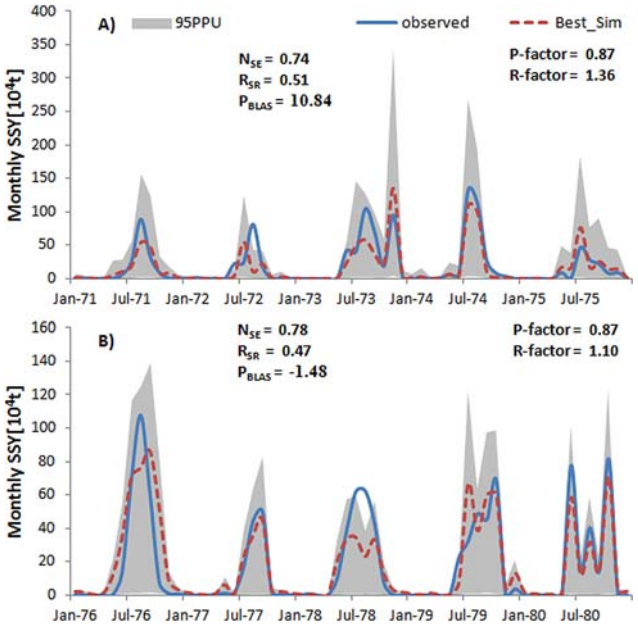

Figure 6. Comparison of the observed monthly suspended sediment yield (blue bold line) and simulated monthly suspended sediment yield (red dashed line) with 95 % prediction uncertainty band at the Kejie hydrological station. Calibration and validation results are shown in Fig. 6a and b.

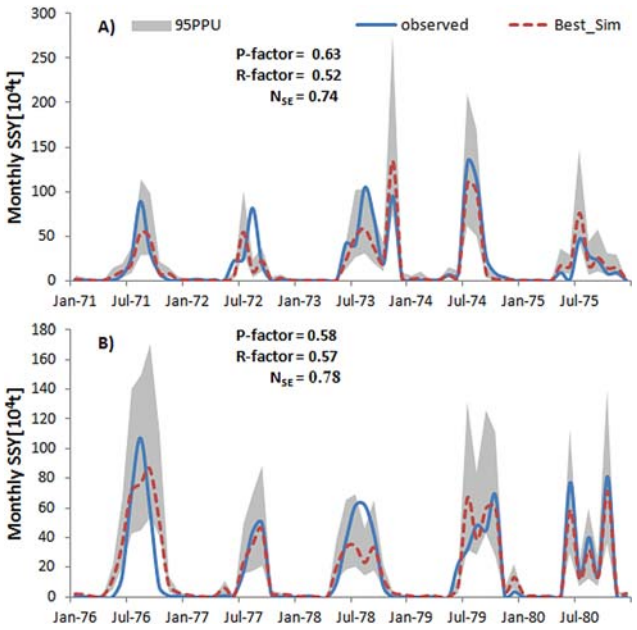

Figure 7. The results for behavioral parameters on the 95 % monthly suspended sediment prediction uncertainty band at the Kejie hydrological station. Calibration and validation results are shown in Fig. 7a and b.

monthly SSY could be bracketed by the 95PPU with a wide 95PPU band of 1.10 (1.36) (out of a perfect 0, but quite reasonable around 1) in the calibration (validation) period. Usually a higher P-factor will cause a higher R-factor. Behavioral solutions can reduce the P-factor and the R-factor, and get a smaller prediction uncertainty in the SUFI-2. The results of behavioral parameters on sediment simulation were shown in Fig. 7a and b. When the 95PPU band is reduced to 0.52 (0.57), 63 % (58 %), respectively, the measured monthly SSY could be bracketed by the 95PPU in the calibration (validation) period. Consequently, the model performance with final parameter ranges (Table 4), as represented by the P-factor and the R-factor, is quite reasonable. The fitting values are the "best" parameter set of the last iteration step with a maximum N_{SE} coefficient.

4.3 Partitioning observed change

4.3.1 Contributions of different factors to SSY

Three scenarios, namely SimulatedL1C1, SimulatedL1C2, and SimulatedL2C2, were produced using the calibrated parameters in the SWAT model. Table 5 lists the mean annual observed SSY and the mean annual simulated values over Period 1 and Period 2.

From Period 1 to 2, the mean annual SSY decreased by 40 % (95.6×10^4 t yr^{-1}) under the joint impacts of human activities and climate change (Table 6), by 18.9×10^4 t yr^{-1} under the impact of climate change, by 45.7×10^4 t yr^{-1} under the impact of land cover change, and by 24.9×10^4 t yr^{-1} under the impact of other engineering measures.

Table 5. Simulated and measured annual suspended sediment yield in the Kejie watershed (1970–2010).

			Mean annual SSY (10^4t yr^{-1})
Measured 1	Period 1	1971–1985	240.8
Measured 2	Period 2	1986–2010	145.2
SimulatedL1C1	Period 1	1971–1985	216.7
	Land-use	Lus1974	
SimulatedL1C2	Period 2	1986–2010	206.7
	Land-use	Lus1974	
SimulatedL2C2	Period 2	1986–2010	161.0
	Land-use	Lus1991 + lus2001 + lus2006 + lus2009	

The decrease in the mean annual SSY from Period 1 to Period 2 was 47.8 % attributable to land cover change, 19.8 % to climate change (a milder rainfall regime), and 26.1 % to other engineering measures. The bias from the model simulation accounted for 6.3 % of the observed change (Table 6).

4.3.2 Effects of climate change

Rainfall is the major driving factor controlling soil erosion. Sediment processes in the watershed are influenced by the intensity, amount, and distribution of rainfall. While the observed declining trend in annual rainfall in the watershed over 1971–2010 was not statistically significant, high interannual variability was observed at the two rainfall sites inside the watershed, ranging from −40 % (2009) to 43.9 % (2001) at the Beimiao site, and from −43.7 % (2009) to 36.3 % (1976) at the Kejie site (Fig. 8). The higher variability in annual rainfall causes the higher variability in the predicted soil erosion. In terms of the average annual rainfall over the two periods, the value over Period 2 decreased by 6.8 % and 6.1 % at the two corresponding sites. Although the trend in rainfall is not statistically different from what can be expected for a no-change hypothesis, the predicted sediment yield is more sensitive to rainfall change than to water discharge (Lu et al., 2013).

SSY is influenced by temperature change indirectly (i.e., temperature change will influence the runoff, which will in turn cause the change of the sediment transportation capacity; its influence on vegetation and weathering will subsequently change the soil erosion rate). Harrison (2000) found temperature was exponentially related to the erosion rate, and Syvitski et al. (2003) indicated there was a negative relationship between temperature and sediment load in a tropical zone. Zhu et al. (2008) predicted the sediment flux would decrease by 1.7 % if the temperature increased by 1 °C in the

Table 6. Contribution of vegetation restoration, climate change and other engineering measures to suspended sediment between Period 1 and Period 2 in the Kejie watershed.

Components	Formulas	Change of annual SSY	
		(10^4 t yr^{-1})	%
Observed change	Measured2-Measured1	−95.6	
Climate effects	SimulatedL1C2-SimulatedL1C1	−18.9	19.8
Land-use change effects	SimulatedL2C2-SimulatedL1C2	−45.7	47.8
Engineering effects	(Measured2-SimulatedL2C2)-Bias in P2	−24.9	26.1
Model bias	Bias in P2 – Bias in P1	−6.0	6.3
Simulation bias			
Bias	Formulas	(10^4 t yr^{-1})	%
Bias in P1	(Measured1-SimulatedL1C1)	15.2	
Percent bias in P1	(Measured1-SimulatedL1C1)/Measured1		6.3
Bias in P2	Measured2*Percent Bias in P1	9.2	

Note: P1 is Period 1 (1971–1985); P2 is Period 2 (1986–2010). L1 is the land cover in Period 1; L2 is the land cover in Period 2. C1 is the climate condition in Period 1; C2 is the climate condition in Period 2. SSY is the suspended sediment yield.

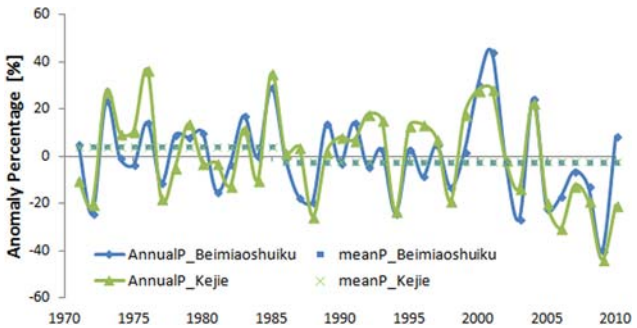

Figure 8. The inter-annual variability of annual rainfall recordings at two stations (Beimiaoshuiku and Kejie from 1971 to 2010). Note: Annual P represents the annual rainfall and mean P the average annual rainfall for the two periods.

Longchuanjiang basin (Yunnan Province). Ma et al. (2009a) described a monotonic increasing trend in the average annual temperature of 0.41 °C (10 yr^{-1}) for the period starting from 1965 in the Kejie watershed. The average annual T_{mean} (the mean temperature), T_{max} (the maximum temperature), and T_{min} (the minimum temperature) increased by 0.9 °C, 0.7 °C and 1.3 °C, respectively, from Period 1 to Period 2. The increase of temperature may contribute to the decrease of the SSY in the Kejie watershed.

A climate change scenario was assumed with a temperature increase of 1 °C and rainfall decrease of 6 % according to the trend between Period 2 and Period 1. The scenario was simulated in the calibrated SWAT model. The result indicates the mean annual SSY will decrease by 14 %. This assumed result explained the reasonable contribution (20 %) of climate change to the SSY reduction from Period 1 to Period 2.

Table 7. Percent of land cover types in the Kejie watershed (1974–2009).

Type	1974	1991	2001	2006	2009
Forest	21.9	34.5	37.3	44.3	55.8
Grassland	28.1	24.5	17.0	12.7	3.4
Cropland	27.0	23.7	26.0	20.4	32.0
Settlement	3.3	3.5	4.2	5.8	5.3
Barren land	18.9	13.1	14.7	16.2	2.9
Water	0.8	0.8	0.9	0.6	0.5

4.3.3 Effects of vegetation restoration

The land-use and land cover in the Kejie watershed (along with many other regions in China) have dramatically changed in the past four decades. The land cover maps of five observations were illustrated in Fig. 9, and the corresponding land cover estimates are summarized in Table 7. The percent of cover represented by forest, cropland, and human settlement increased by 33.9 %, 5.0 %, and 2.0 %, respectively, while the area of grassland and barren land declined by 24.6 % and 15.9 %, respectively, from 1974 to 2009, with small variations in what was identified as open water.

The increase of forest in the Kejie watershed (from 21.9 % to 55.8 %) can be directly attributed to the forestry management policies of the central government in China which were implemented over the past several decades. Aerial seeding reforestation efforts started in 1987, and were followed by two large-scale conservation programs – namely, the Natural

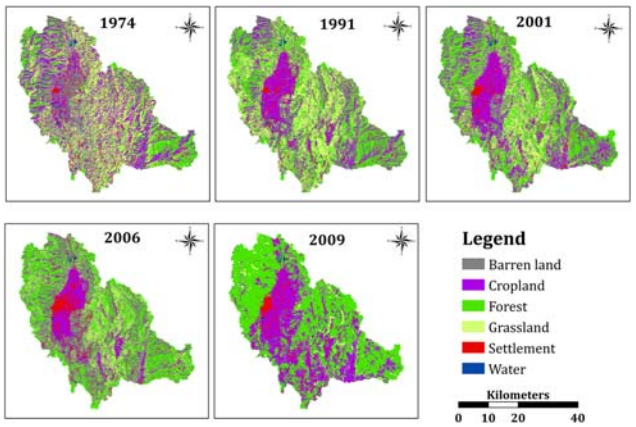

Figure 9. The land-use and land cover maps in the Kejie watershed (1974–2009).

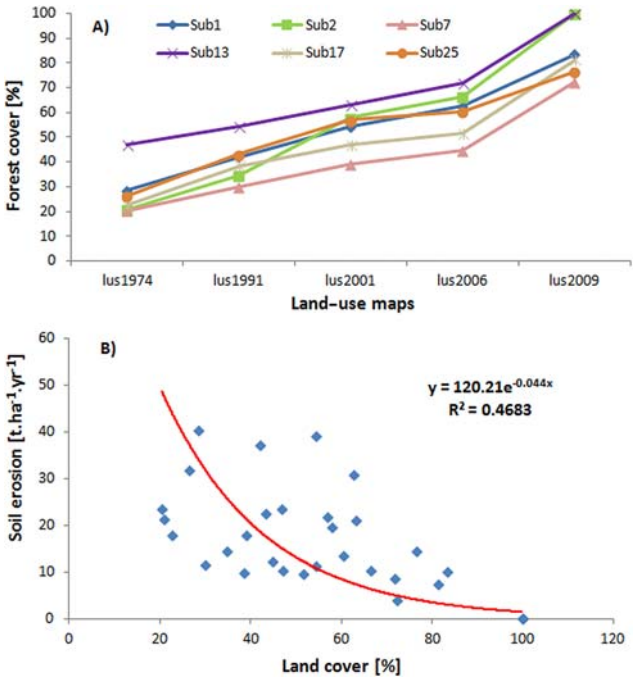

Figure 10. Relationship between forest cover and soil erosion at the six sub-basins (Fig. 10b) with similar forest cover change trend (Fig. 10a) in the Kejie watershed (1974–2009).

Forest Protection Program (NFPP) and the Grain for Green Project (GGP, but originally called the Sloping Land Conversion Program). The NFPP was introduced in 1998 to rehabilitate and develop natural forests (Zhang et al., 2000). GGP started in 1999, and aimed to restore the landscape by paying farmers to plant trees rather than crops (Wang et al., 2007a). The forest cover in China as a whole increased from 16.6 % to 18.2 % in 2005, and the goal is to reach 26 % by 2050 (Wang et al., 2007a). Yunnan Province was the priority for NFPP and was also in the priority areas of GGP.

The increase of forest can also be attributed to several soil and water conservation programs initiated in the Kejie watershed. The first soil and water conservation program in Yunnan Province was started in 1989 as part of a National Key Soil Conservation Project supported by the central government of China (Wei et al., 2011). After that, several other soil and water conservation programs were launched, such as the Yangtze River treatment project, the Pearl River treatment project, and the Treasury bond projects supported by the central government (Ma et al., 2009b). Ecological and engineering measures have been undertaken in all of these programs.

For the sake of local inventory data, which was provided by the Baoshan Water Conservancy Bureau, five soil and water conservation projects (located in the Ajiadahe, Binmawahe, Longwangmiao, Santaizihe and Wadudahe basins), ranging in area between 20.36 and 27.87 km^2, were implemented in the Kejie watershed from 2000 to 2005. Consequently, the soil erosion area was reduced by 40–81 %. The effect of the different measures on soil erosion was estimated using the empirical formulas (Table 8). In terms of ecological measures, the reduction of soil loss was estimated by the treatment areas and multiplied by an empirical coefficient, which indicates how much soil loss will be reduced by implementing a hectare of a specific treatment. Generally speaking, the contribution from ecological measures (ecological forest for soil and water conservation; and economical forest for fruits and nuts) was around 41 %.

To further explore the effect of vegetation restoration on SSY, six sub-basins with similar land cover and land-use change trends were selected from the watershed (Fig. 10a). The total area was 421.8 km^2, with sub-basin size ranging from 35.8 km^2 to 133.1 km^2. The five soil and water conservation programs at the Ajiadahe, Binmawahe, Longwangmiao, Santaizihe and Wadudahe basins were located in sub-basins 1, 25, 2, 7, and 17, respectively. We assumed that the land cover in the Kejie watershed changed during the periods 1974 to 1991, 2001, 2006 and 2009 in Period 1 (1971–1985), respectively. The annual soil erosion (1971–1985) from six sub-basins under five land-use maps was simulated using the calibrated and validated SWAT model. When the land cover changed from the 1974 map to the 2009 map, the reduction in the soil erosion ranged between 10.5 and 30.2 $t\,ha^{-1}\,yr^{-1}$ among six sub-basins. The relationship between the forest cover and soil erosion was illustrated in Fig. 10b. An exponential relationship between the forest cover and soil erosion represents the data adequately. The relationship implies vegetation restoration can effectively control soil erosion in these watersheds.

4.3.4 Effects of engineering measures

Except for the ecological forest for soil and water, conservation, and economical forest for fruit and nuts, the major

Table 8. The contribution of ecological and engineering measures to soil loss reduction at four plot sites (2000–2005).

	Measures	Contribution to soil loss reduction (%)			
		No1	No2	No3	No4
Ecological measures	Ecological forest for soil and water conservation	47.5	27.3	35.4	37.0
	Economical forest for fruits and nuts	1.7	1.1	5.1	7.3
	Closed treatment	24.2	12.0	3.6	8.3
	Conservative tillage	6.7	5.5	3.6	4.2
Engineering measures	Terrace	15.0	5.5	4.4	5.2
	Silt check dam	5.0	48.6	47.8	38.0

Notes: No 1= Ajiadahe basin; No2 = Binmawahe basin; No3 = Santaizihe Basin; No4 = Wadudahe basin.

Table 9. The potential disposal of excavated soil, as well as investment in soil and water conservation by construction projects (2004–2010).

Year	Protect area (ha)	Waste soil ($10^4 m^3$)	Investment on soil and water conservation (10^4 RMB)
2004	8.7	6.5	16.2
2005	15.0	1.1	154.5
2006	38.8	11.4	576.6
2007	1267.9	1607.3	203.6
2008	7.6	91.8	3.0
2009	4.9	1.6	51.2
2010	372.6	187.7	1773.0
Sum	1715.5	1907.3	2778.1

Note: RMB: Chinese Currency, Ren Ming Bi.

measures taken in the programs included closed treatment, conservative tillage, and terrace and silt check damming. The effect of terrace measures on soil erosion was estimated using the similar experimental formula of ecological measures. In terms of silt check dams, the reduction of soil loss was simply estimated using the number of silt check dams to multiply by one empirical coefficient derived from previous work, which indicated the capacity of a silt check dam to reduce soil loss. From Table 8, the contribution from engineering measures, plus closed-treatment and conservative tillage, was around 59 %. The value had high uncertainty, as the assessment method was somewhat subjective and lacked details of the routing processes of sediment from the plot to watershed level.

Several construction projects were implemented in the watershed during the previous decades, which led to soil wasting (Table 9). From 2004 to 2010, a total of 1907.3×10^4 m^3 waste soil from construction sites was treated properly, as a key measure to prevent soil and water losses.

Additionally, several sand mining plants actively take sand from the Donghe River. It was difficult to quantify the amount of sand taken, as the plants lacked legal licensing and operated irregularly.

It is also important to note that, during the past several decades, in order to prevent (and hopefully) eliminate the risk of flood disasters, the riverbanks of the Donghe in the upperstream regions were reconstructed with concrete, which also may have had some unspecified effect on sediment transfer.

The SSY in the Kejie watershed during Period 2 was influenced by all these kinds of engineering measures. It is difficult to assess the specific effect of all these measures on soil erosion accurately. Meanwhile, it is also difficult to consider these measures when using a hydrological model to simulate the SSY. The difference between the simulated SSY without considering engineering measures and the observed SSY minus the simulation bias is an alternative way to estimate the effect of the engineering measures on SSY at the watershed level, although the simulated values contained some uncertainty in the hydrological modeling.

5 Discussion

The sediment generation and transportation in the watershed is a comprehensive process which is influenced by human activities and climate change. Yet, it is a challenge to quantify the effects from different factors. The SWAT model is widely used to simulate the sediment process with satisfying results (Qiu et al., 2012, and Shrestha et al., 2013). The SWAT model was set up successfully and the contribution from climate change (19.8 %), vegetation restoration (47.8 %) and other engineering measures (26.1 %) to the sediment reduction were differentiated in our study.

There are some uncertainties in any modeling method, including input data, model structure, model parameters, and the measured data. It is necessary, therefore, to do uncertainty analysis when conducting hydrological modeling. In our study, the input data uncertainty is from rainfall data and

land cover maps. There are 13 rainfall stations available over different record periods, and 8 of them are concentrated in the Xizhuang sub-watershed area. The distribution of rainfall gauges can not describe rainfall spatial distribution accurately, especially in the mountainous area. Consequently, the land-use maps were derived from satellite images combining ground control points. The uncertainties of the land-use maps in 1974, 1991, 2001 and 2006 were analyzed by Ma et al. (2009a). The map in 2009 was obtained from a different source which also contained some uncertainty. In terms of model structure, the weakness of the SWAT model is that it cannot track the specific peak runoff and sediment yield more accurately because some empirical equations are used inside the model (i.e., the SCS, CN, and MUSLE). With that in mind, the peak runoff and sediment are usually underestimated. The sediment parameters in the SWAT model are not well defined physically; no measurements are available to estimate the parameters (Qiu et al., 2012). The observed discharge and suspended sediment data are obtained from the hydrological station where all the data have been cross-checked. However, there is still some uncertainty, including the numbers of soil water samples taken during the discharge events. Obviously, it is difficult to consider uncertainty from each source separately, so SUFI-2 was used to analyze the SWAT modeling uncertainty in our study.

The results from SUFI-2 indicate the uncertainties of the sediment modeling with final parameter ranges are within reasonable ranges: 95PPU captured more than 60 % of the observed monthly SSY with a narrower band (about 0.52). The statistics of N_{SE}, R_{SR} and P_{BLAS} in the sediment simulation with the best parameter from the final parameter ranges indicated a reasonably trustworthy result. Therefore, the contribution ratio of climate change, vegetation restoration, and other engineering measures are within acceptable uncertainty levels.

Additionally, to some limited extent, the climate change scenario simulation has tested the contributions of climate change to sediment reduction. The increasing temperature and the high inter-annual variability of annual rainfall are the main climatic factors determining the sediment reduction. A comparison of the contributions of climate change and human activities showed that human activities were a governing factor for river sediment delivery, which coincides with the findings of Dai et al. (2009) in China. The vegetation restoration and engineering measures described in Sect. 4 provide evidential proof to account for the contribution of human activities to sediment reduction. The dominant contribution of the vegetation restoration was explained by the exponential relationship between the forest cover and soil erosion at the sub-watershed level.

6 Conclusions

The annual suspended sediment decreased significantly in the Kejie watershed (from 13.7 t ha^{-1} yr^{-1} to 8.3 t ha^{-1} yr^{-1}) between the period 1971–1985 and the period 1986–2010. At the same time, there has been no apparent decreasing trend observed for the annual runoff, which seems to indicate other factors are controlling sediment decrease in the watershed.

The SWAT model was auto-calibrated using SUFI-2 program. Although there was some uncertainty in the sediment simulation, the results indicate the modeling captured 63 % (58 %) of the measured SSY with 0.57 (0.52) of 95PPU band width in the calibration (validation) period. The simulation with fitting values (best parameters) showed a high N_{SE} value and a low P_{BLAS}, so we believe the simulation results from the SWAT model are reasonable.

The subsequent results show a larger contribution of land-use/cover change to the reduction in suspended sediment yield (relative to engineering and other human activities), than the majority of previous studies on this subject elsewhere in China. The sharp decrease in sediment yield from 1985, although assisted by a milder rainfall regime, was mostly due to the effects of more than 10 years of reforestation (forest cover increasing from 21.9 % to 55.8 %), as well as soil and water conservation efforts. Since 1985, the health and stability of the river ecosystem seems to have significantly improved.

Acknowledgements. This research is part of CGIAR's Research Program 6 (Forests, Trees and Agroforestry), and IDRC, Canada, supported project on "Building Effective Water Governance in the Asian Highlands". We also would like to express our sincere gratitude to the Baoshan Water Conservancy Bureau and the Baoshan Meteorological Bureau for their data support.

Edited by: T. Bogaard

References

Abbaspour, K. C., Yang, J., Maximov, I., Siber, R., Bogner, K., Mieleitner, J., Zobrist, J., and Srinivasan, R.: Modelling hydrology and watetr quality in the pre-alpine/alpine Thur watershed using SWAT, J. Hydrol., 333, 413–430, 2007.

Abbaspour, K. C., Faramarizi, M., Ghasemi, S. S., and Yang, H.: Assessing the impact of climate change on water resources in Iran, Water Resour. Res., 45, 1–16, 2009.

Arnold, J. G. and Fohrer, N.: SWAT2000: current capabilities and research opportunities in applied watershed modelling, Hydrol. Process., 19, 563–572, doi:10.1002/hyp.5611, 2005.

Arnold, J. G., Williams, J. R., and Maidment, D. R.: Continuous-Time Water and Sediment-Routing Model for Large Basins, J. Hydraul. Eng.-ASCE, 121, 171–183, doi:10.1061/(ASCE)0733-9429(1995)121:2(171), 1995.

Azimi, M., Heshmati, Gh. A., Farahpour, M., Faramarzi, M., and Abbaspour, K. C.: Modeling the impact of rangland management

on forage production of sagebrush species in arid and semi-arid regions of Iran, Ecol. Model., 250, 1–14, 2013.

Bagnold, R. A.: Bed load transport by natural rivers, Water Resour. Res., 13, 303–312, doi:10.1029/WR013i002p00303, 1977.

Betrie, G. D., Mohamed, Y. A., van Griensven, A., and Srinivasan, R.: Sediment management modelling in the Blue Nile Basin using SWAT model, Hydrol. Earth Syst. Sci., 15, 807–818, doi:10.5194/hess-15-807-2011, 2011.

Burn, D. H., Cunderlik, J. M., and Pietroniro, A.: Hydrological trends and variability in the Liard River basin / Tendances hydrologiques et variabilité dans le basin de la rivière Liard, Hydrol. Sci. J., 49, 53–67, doi:10.1623/hysj.49.1.53.53994, 2004.

Cai, T., Li, Q. F., Yu, M. X., Lu, G. B., Cheng, L.P., and Wei, X.: Investigation into the impacts of land-use change on sediment yield characteristics in the upper Huaihe River basin, China, Phys. Chem. Earth, 53–54, 1–9, doi:10.1016/j.pce.2011.08.023, 2012.

Dai, S. B., Lu, X. X., Yang, S. L., and Cai, A. M.: A preliminary estimate of human and natural contributions to the decline in sediment flux from the Yangtze River to the East China Sea, Quat. Int., 186, 43–54, doi:10.1016/j.quaint.2007.11.018, 2008.

Dai, S. B., Yang, S. L., and Li, M.: The sharp decrease in suspended sediment supply from China's rivers to the sea: anthropogenic and natural causes, Hydrol. Sci. J., 54, 135–146, doi:10.1623/hysj.54.1.135, 2009.

Faramarzi, M., Abbaspour, K .C., Schulin, R., and Yang, H.: Modelling blue and green water resources availability in Iran, Hydrol. Process., 23, 486–501, 2009.

Hairiah, K., Sulistyani, H., Suprayogo, D., Widianto, Purnomosidhi, P., Widodo, R. H., and Van Noordwijk, M.: Litter layer residence time in forest and coffee agroforestry systems in Sumberjaya, West Lampung, Forest Ecol. Manag., 224, 45–57, doi:10.1016/j.foreco.2005.12.007, 2006.

Harrison, C. G. A.: What factors control machanical erosion rates? Int. J. Earth Sci., 88, 752–763, 2000.

Huang, M. B. and Zhang, L.: Hydrological responses to conservation practices in a catchment of the Loess Plateau, China, Hydrol. Process., 18, 1885–1898, doi:10.1002/hyp.1454, 2004.

Kendall, M. G.: Rank Correlation Methods, Oxford, England, Griffin, 1948.

Liu, C., Sui, J., and Wang, Z. Y.: Sediment load reduction in Chinese rivers, Int. J. Sediment Res., 23, 44–55, doi:10.1016/S1001-6279(08)60004-9, 2008.

Lu, X. X., Ran, L. S., Liu, S., Jiang, T., Zhang, S. R., and Wang, J. J.: Sediment loads response to climate change: A preliminary study of eight large Chinese rivers, Int. J. Sediment Res., 28, 1–14, doi:10.1016/S1001-6279(13)60013-X, 2013.

Ma, X., Xu, J. C., Luo, Y., Prasad Aggarwal, S., and Li, J. T.: Response of hydrological processes to land-cover and climate changes in Kejie watershed, south-west China, Hydrol. Process., 23, 1179–1191, doi:10.1002/hyp.7233, 2009a.

Ma, X., Zhu, X., and Zhao, R.: Index system of DPSIR framework for soil erosion in Yunnan Province, Environmental Science Survey, 28, 1–5, 2009b (in Chinese).

Mann, H. B.: Nonparametric tests against trend, Econometrica, 13, 245–259, 1945.

Men, G. T.: Treatment and benefit analysis on water and soil loss in Yunnan Province, China, Soil and Water Conservation in China, 2, 34–36, 2011 (in Chinese).

Moriasi, D. N., Arnold, J. G., Van Liew, M. W., Bingner, R. L., Harmel R. D., and Veith, T. L.: Model evaluation guidelines for systematic quantification of accuracy in watershed simulations, Trans. ASAE, 50, 885–900, 2007.

Neitsch, S. L., Arnold, J. G., Kiniry, J. R., Srinivasan, R., and Williams, J. R.: Soil and Water Assessment Tool User's Manual: Version 2000, Texas Water Resources Institute, College Station, Texas TWRI Report TR-192, 2002.

Oeurng, C., Sauvage, S., and Sánchez-Pérez, J.-M.: Assessment of hydrology, sediment and particulate organic carbon yield in a large agricultural catchment using the SWAT model, J. Hydrol., 401, 145–153, 2011.

Oswald, C. J., Richardson, M. C., and Branfireun, B. A.: Water storage dynamics and runoff response of a boreal Shield headwater catchment, Hydrol. Process., 25, 3042–3060, doi:10.1002/hyp.8036, 2011.

Pimentel, D.: Soil Erosion: A Food and Environmental Threat, Environ. Dev. Sustainability, 8, 119–137, doi:10.1007/s10668-005-1262-8, 2006.

Qiu, L. J., Zheng, F. L., and Yin, R. S.: SWAT-based runoff and sediment simulation in a small watershed, the loessial hilly-gullied region of China: capabilities and challenges, Int. J. Sediment Res., 27, 226–234, doi:10.1016/S1001-6279(12)60030-4, 2012.

Ran, D. C., Luo, Q. H., Zhou, Z. H., Wang, G. Q., and Zhang, X. H.: Sediment retention by check dams in the Hekouzhen-Longmen Section of the Yellow River, Int. J. Sediment Res., 23, 159–166, doi:10.1016/S1001-6279(08)60015-3, 2008.

Ran, L. S., Lu, X. X., and Xu, J. C.: Effects of vegetation restoration on soil conservation and sediment loads in China: A critical review, Crit. Rev. Env. Sci. Tec., 43, 1384–1415, 2013.

Rijsberman, F. R., and Wolman, M. G.: Effect of erosion on soil productivity: an international comparison, J. Soil Water Conserv., 40, 349–354, 1985.

Schuol, J., Abbaspour, K. C., Yang, H., Srinivasan, R., and Yang, H.: Estimation of freshwater availability in the west Africa subcontinent using the SWAT hydrologic model, J. Hydrol., 352, 30–49, 2008a.

Schuol, J., Abbaspour, K. C., Yang, H., Srinivasan, R., and Zehnder, A. J. B.: Modeling blue and green water availability in Africa, Water Resour. Res., 44, 1–18, 2008b.

Shrestha, B., Babel, M. S., Maskey, S., van Griensven, A., Uhlenbrook, S., Green, A., and Akkharath, I.: Impact of climate change on sediment yield in the Mekong River basin: a case study of the Nam Ou basin, Lao PDR, Hydrol. Earth Syst. Sci., 17, 1–20, doi:10.5194/hess-17-1-2013, 2013.

Syvitski, J. P. M., Pechham, S. D., Hilberman, R., and Mulder, T.: Predicating the terrestrial flux of sediment to the global ocean: a planetary perspective, Sediment. Geol., 162, 5–24, 2003.

Tang, L. H., Yang, D. W., Hu, H. P., and Gao, B.: Detecting the effect of land-use change on streamflow, sediment and nutrient losses by distributed hydrological simulation, J. Hydrol., 409, 172–182, 2011.

Team, R. C.: R: A language and environment for statistical computing, Vienna, Austria: R Foundation for Statistical Computing, 1–1731, 2008.

Toms, J. D. and Lesperance, M. L.: Piecewise regression: a tool for identifying ecological thresholds, Ecology, 84, 2034–2041, 2003.

van Belle, G. and Hughes, J. P.: Nonparametric Tests for Trend in Water Quality, Water Resour. Res., 20, 127–136, doi:10.1029/WR020i001p00127, 1984.

Verbist, B., Poesen, J., van Noordwijk, M., Suprayogo, D., Agus, F., and Deckers, J.: Factors affecting soil loss at plot scale and sediment yield at catchment scale in a tropical volcanic agroforestry landscape, Catena, 80, 34–46, 2010.

Walling, D. E. and Fang, D.: Recent trends in the suspended sediment loads of the world's rivers, Global Planet. Change, 39, 111–126, 2003.

Wang, G. Y., Innes, J. L., Lei, J. F., Dai, S. Y., and Wu, S. W.: China's forestry reforms, Science, 318, 1556, doi:10.1126/science.1147247, 2007a.

Wang, H. J., Yang, Z. S., Saito, Y., Liu, J. P., Sun, X. X., and Wang, Y.: Stepwise decreases of the Huanghe (Yellow River) sediment load (1950–2005): Impacts of climate change and human activities, Global Planet. Change, 57, 331–354, 2007b.

Wei, J., He, X. B., and Bao, Y. H.: Anthropogenic impacts on suspended sediment load in the Upper Yangtze river, Reg. Environ. Change, 11, 857–868, 2011.

Williams, J. R.: SPNM, a model for predicting sediment, phosphorous, and nitrogen yields from agricultural basin, J. Am. Water Resour. As., 16, 843–848, 1980.

Williams, J. R. and Berndt, H. D.: Sediment yield prediction based on watershed hydrology, Trans. ASAE, 20, 1100–1104, 1977.

Wu, C. S., Yang, S. L., and Lei, Y. P.: Quantifying the anthropogenic and climatic impacts on water discharge and sediment load in the Pearl River (Zhujiang), China (1954–2009), J. Hydrol., 452, 190–204, 2012.

Xu., X. Z., Zhang, H. W., and Zhang, O. Y.: Development of check-dam systems in gullies on the Loess Plateau, China, Environ. Sci. Policy, 7, 79–86, doi:10.1016/j.envsci.2003.12.002, 2004.

Xiong, M., Xu, Q. X., and Yuan, J.: Analysis of multi-factors affecting sediment load in the Three Gorges Reservoir, Quat. Int., 208, 76–84, 2009.

Xu, Y. D., Fu, B. J., and He, C. S.: Assessing the hydrological effect of the check dams in the Loess Plateau, China, by model simulations, Hydrol. Earth Syst. Sci., 17, 2185–2193, doi:10.5194/hess-17-2185-2013, 2013.

Zhang, G. L., Zhang, Y. J., Dong, J. W., and Xiao, X. M.: Green-up dates in the Tibetan Plateau have continuously advanced from 1982 to 2011, P. Natl. Acad. Sci. USA, 110, 4309–4314, 2013.

Zhang, J. G., Hu, B. H., Ruan, H., and Fang, Y. M.: The present situation and control measures of soil and water loss in Changjiang River valley, Journal of Nanjing Forestry University, 23, 17–21, 1999 (in Chinese).

Zhang, P. C., Shao, G. F., Zhao, G., Le Master, D. C., Parker, G. R., Dunning, J. B., and Li, Q. L.: China's forest policy for the 21st century, Science, 288, 2135–2136, doi:10.1126/science.288.5474.2135, 2000.

Zhou, J., Liu, Y., Guo, H. C., and He, D.: Combining the SWAT model with sequential uncertainty fitting algorithm for streamflow prediction and uncertainty analysis for the Lake Dianchi Basin, China, Hydrol. Process., 28, 521–533, 2014.

Zhu, Y. M., Lu, X. X., and Zhou, Y.: Sediment flux sensitivity to climate change: A case study in the Longchuanjiang catchment of the upper Yangtze River, China, Global Planet. Change, 60, 429–442, 2008.